Light Assisted Dimer to Monomer Transformation in Heavily Doped Rhodamine 6G−Porous Silica Hybrids

Carlo M. Carbonaro,*,† Franco Meinardi,‡ Pier C. Ricci,† Marcello Salis,† and Alberto Anedda†,§

Dipartimento di Fisica, Università di Cagliari, Cittadella Universitaria, S.P. no. 8, I-09042 Monserrato, Cagliari, Italy, INFM and Dipartimento di Scienza dei Materiali, Università Milano-Bicocca, Via Cozzi 53, I-20125 Milano, Italy, and CGS, Centro Grandi Strumenti, Università di Cagliari, S.P. no. 8, km 0.700, 09042, Monserrato, Italy

Received: December 9, 2008; Revised Manuscript Received: February 19, 2009

The spectral properties of postdoping prepared type I Rhodamine 6G−silica hybrids were investigated in the case of intentionally large doping (5×10^{-2} mol/L). Beside expected concentration quenching effects, steady state and time resolved optical spectroscopy measurements displayed the presence of different kind of aggregates, both fluorescent and nonfluorescent. As the irradiation dose on the sample increases, the emission features change: the overall emission increases, the peak of the emission is blue-shifted, and the emission decay time also increases. The modifications of the spectral properties under light excitation are interpreted in terms of dimer to monomer light assisted transformation, and a thermodynamic model based on a monomolecular kinetics is presented.

1. Introduction

The sol−gel technique allows easy incorporation of organic dyes into the transparent matrix of porous silica for technological applications ranging from luminescent solar collectors to solid state lasers.[1−10] One of the main advantages of the organic−inorganic hybrids compared to liquid solutions is that the concentration effects reported for the second ones are expected at larger dye concentrations.[6] Indeed as the dye concentration increases, the distance between monomer species of the dye molecules observed in diluted systems is reduced and aggregate species, such as dimers and/or oligomers, can be formed.[11] The use of the inorganic matrix allows isolation of dye molecules up to larger concentrations than in liquid solutions and reduction of the collisional deactivation mechanisms. Thus the effects of the concentration can be studied in a system with reduced mobility.[6]

The formation of different kinds of dye aggregates depends both on the synthesis method and on the coupling between the organic dye and the inorganic matrix.[12,13] From a technological point of view the investigation of the concentration limit of hybrid samples and the characterization of the spectroscopic features of samples with different contents of dye molecules are important issues to be addressed. As an example, an increased time and spectral tunability was recently reported for xanthene doped silica matrixes and related to the formation of fluorescent dimers.[12−18] On the other hand, one of the main drawbacks of large doping of inorganic matrixes is the reduced capability of the dye molecules to dissipate the accumulated energy because of their reduced mobility: the fast degradation of the dye molecules leads to the decrease in the emission performance of the hybrid sample as the irradiation dose increases. The specific kinetics of the decrease of the emission performance depends on the thermal properties of the inorganic matrix and the guest−host interactions.[19−24] In addition, external conditions such as the local temperature and the excitation power affect the dye photostability.[25] The main mechanisms leading to the photodegradation of the molecules are the oxidation process and multiphoton ionization.[26−29] In a recent paper[30] we reported that the photobleaching of sol−gel prepared hybrid samples depends on the mobility of the dye molecules: isolated molecules are characterized by a larger photostability than nonisolated tumbling molecules. At the concentration limit the density of isolated molecules is strongly reduced and the photophysics of the dimer species can be investigated in detail. In this paper we report the analysis of Rhodamine 6G (Rh6G) doped porous silica samples prepared by postdoping impregnation of sol−gel synthesized commercial porous silica. The chosen concentration was 5×10^{-2} mol/L, far beyond the reported concentration limit of a comparable liquid solution.[31] The absorption and photoluminescence (PL) properties of the investigated samples indicated the expected concentration effects due to the formation of different kinds of dye aggregates, such as the observation of different absorption bands and the observation of the emission band of the fluorescent dimers. However, instead of the well-documented photobleaching phenomena,[19−24,26−30] as the irradiation dose increased we observed the increase of the emission intensity and its spectral modification. Data are interpreted based on the scheme of the molecular exciton theory, and the light assisted transformation of dimer to monomer species of the dye molecules is reported. A monomolecular model for the kinetics of the dimer to monomer light assisted transformation is presented.

2. Experimental Methods

Time resolved photoluminescence measurements were carried out in the picosecond to nanosecond time range by exciting the samples with the second harmonic of a Coherent Ti:sapphire laser (excitation wavelength 355 nm, 200 fs pulse duration, repetition rate 76 MHz). The mean power density was 2.5

* To whom correspondence should be addressed. E-mail: cm.carbonaro@dsf.unica.it.
† Dipartimento di Fisica, Università di Cagliari.
‡ Università di Milano-Bicocca.
§ CGS, Università di Cagliari.

10.1021/jp810835j CCC: $40.75
Published on Web 03/23/2009

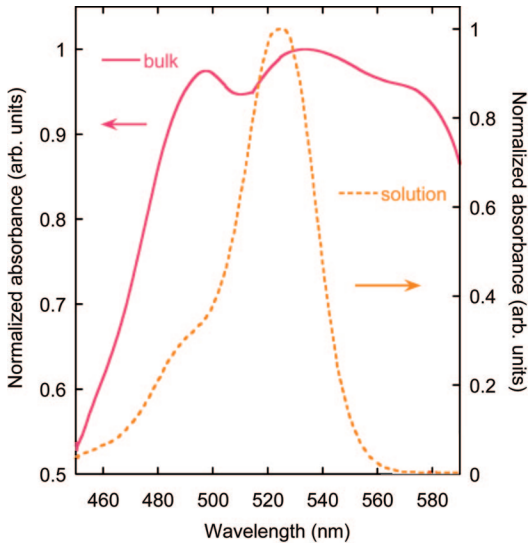

Figure 1. Absorbance spectrum of the hybrid sample. The spectrum of a 5×10^{-6} mol/L methanolic solution of Rh6G is reported for comparison.

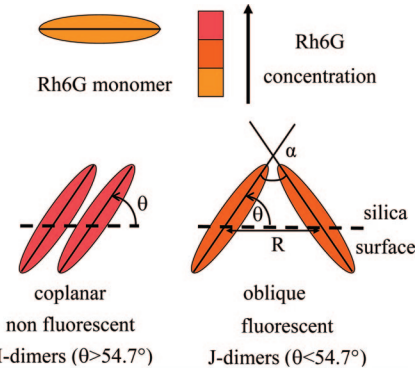

Figure 2. Schematic representation of the dimer formation on the silica surface. Colors are referred to the dye concentration.

W/cm^2, and it was reduced to 0.1 W/cm^2 to perform sequenced PL measurements as a function of the irradiation dose. The signal detection was performed with a Hamamatsu streak camera (Model C5680) coupled with a Cromex spectrograph for the spectral and time resolved measurements (overall system time response shorter than 4 ps, spectral resolution 1 nm).

Absorption measurements were carried out by measuring the light transmitted by the sample with a liquid nitrogen cooled CCD (ISA Jobin Yvon) coupled with a home-designed spectrograph (Dilor-Jobin Yvon).

Emission spectra were recorded with a photonic multichannel analyzer (Hamamatsu PMA-11) excited with three different lines (457.9, 488.0, and 514.5 nm) of a multiline argon ion laser (INNOVA 90C-4). The excitation power density was 2.5 W/cm^2, and the emission spectral resolution was 1 nm.

Type I organic−inorganic samples were prepared by a postdoping technique: commercial porous silica samples (pore diameter 5.4 nm, 5% standard deviation) produced by Geltech Inc., US,[32] were impregnated with Rh6G ethanolic solution (dye concentration 5×10^{-2} mol/L, a 15% error is allowed). Sample impregnation was obtained by capillary absorption, and drying was performed by leaving hybrids in air at standard pressure and temperature. Uniformly colored disks of 5 mm diameter and 3 mm thickness were obtained.

All the emission measurements were carried out in the "front face mode" by collecting the PL signal in the same direction as the reflected excitation beam in order to minimize the reabsorption effects.[12,15−18] When needed, a cutoff filter at 515 nm was applied to remove the excitation source from the PL spectra. All the spectra were corrected for the optical transfer function of the adopted measurement system.

3. Results and Discussion

In Figure 1 the absorbance spectrum of the hybrid sample is reported together with the absorbance spectrum of a dilute Rh6G methanolic solution (Rh6G concentration 5×10^{-6} mol/L) for comparison. The spectrum of the dilute solution shows the typical absorption band at 525 nm related to the monomer form of the dye molecule with a vibrionic shoulder at about 500 nm.[33] The spectrum of the hybrid sample displays three absorption bands at about 500, 530, and 570 nm. Beside the absorption band related to the monomers, the presence of the other two bands and their relative contributions can be explained by considering the formation of dimer aggregates.

The formation of aggregates is related to the interaction among the molecule and the polar surface and other monomers. The fluorescent or nonfluorescent character of the dimers depends on the adsorption geometry on the surface[34,35] which is defined by the angle (θ) formed between the transition dipole moment of each monomer unit and the surface (Figure 2). In the case of $\theta < 54.7°$, the in-plane oblique angle configuration is adopted with an angle (α) among the transition dipole moments of the monomer units such as $\alpha + 2\theta = 180°$. When the transition dipole moments of the monomer units are coplanar, the parallel plane twist angle configuration is realized with $\theta > 54.7°$ (in this configuration $\alpha = 0°$). As explained by molecular exciton theory,[34−37] when dimer aggregates are formed, the absorption band of the two monomers is split to form one band at a higher energy with respect to the absorption band of the monomer (called the H-band) and one band at lower energy (called the J-band). The exciton theory expectation is that the first kind of dimers are fluorescent (J-dimers) and the second ones are nonfluorescent (H-dimers). In addition, the relative contributions of the two absorption bands distinguish the two kinds of aggregates: the transition to the H-band is larger than the transition to the J-band in the parallel plane twist angle model whereas the opposite is observed in the case of in-plane oblique angle model.[34−37] It was also reported that fluorescent dimers of xanthene molecules can be formed at the adsorbed state in a coplanar inclined configuration with $\theta < 54.7°$.[12]

The absorbance spectrum reported in Figure 1 reveals that, besides the monomer species (absorbance band at about 530 nm), a large content of dimer aggregates is formed in the analyzed hybrid sample (absorbance bands at about 500 and 580 nm). A heuristic deconvolution of the absorbance spectrum with three Gaussian bands indicates the absorbance peaks at about 492, 536, and 579 nm respectively, with relative contributions of about 36, 37, and 27% (estimated through the percentage integral area). The slight red shift of the monomer band is related to the presence of the J-band. Since both the H-band and J-band are observed but with a larger contribution of the former, the presence of nonfluorescent H-dimers at the silica surface can be deduced. It should be noted that the obtained value of the exciton splitting ($\Delta\nu = 3064$ cm^{-1}) is in good agreement with the value previously reported for Rh6G doped sol−gel silica ($C_{Rh6G} = 0.32 \times 10^{-3}$ mol/L).[17]

Besides the nonfluorescent H-dimers the presence of a moiety of fluorescent aggregated molecules is deduced by the PL spectra of the samples excited with different excitation wavelengths

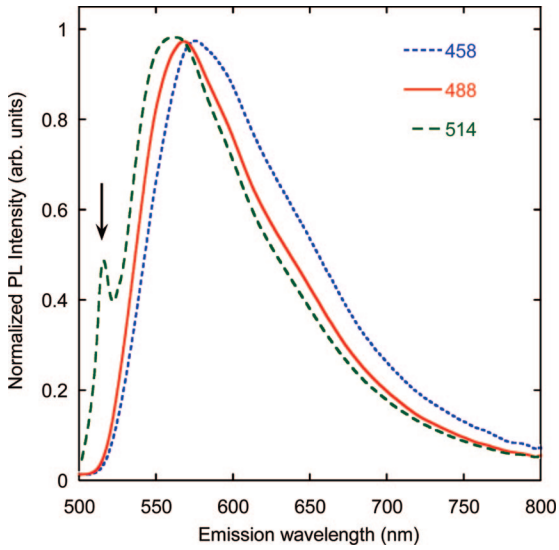

Figure 3. Normalized PL intensity excited at different excitation wavelengths. The arrow indicates the 514.5 nm excitation wavelength only partially suppressed by the filter (GG515).

(457.9, 488.0 and 514.5 nm) and reported in Figure 3 (the arrow indicates the 514.5 nm excitation line only partially suppressed by the filter).

The spectra report the emission band of the monomers at about 550 nm and a shoulder above 610 nm related to the fluorescent dimers.[17] As the excitation wavelength increases, the monomer emission peak blue shifts from 575 to 560 nm because of the presence of different kinds of fluorescent aggregates which have different relative contributions to the emission spectra.[12,15−18] It was reported for xanthene molecules in porous silica that the increase of the dye concentration leads to the formation of fluorescent J-dimers up to a concentration limit above which the fluorescent dimers are gradually converted into nonfluorescent ones.[12,15−18] The reported concentration limit is about 1×10^{-3} mol/L. Data here collected can be interpreted in this context: since the concentration of the investigated sample is 1 order of magnitude larger than the above-reported concentration limit, a large content of H-dimers is expected, as confirmed by the absorbance spectrum. Besides nonfluorescent dimers, the presence of a variety of fluorescent dimers is inferred by the emission spectra and by the blue shift of the emission peak as the excitation wavelength increases.

Figure 4 reports the emission spectrum of the investigated Rh6G porous silica hybrid excited under ultrafast radiation at 355 nm. The emission spectrum is peaked at about 575 nm and displays a full width at half-maximum (fwhm) of about 45 nm. It is worth noting that the fwhm is lower than the width recorded under steady state excitation (of about 90 nm). Concerning the peak position, if one assumes a linear shift of the peak position as a function of the excitation wavelength, as deduced by the steady state measurements (Figure 3), the PL excited at 355 nm should be detected at about 595 nm, whereas the PL recorded under ultrafast excitation at 355 nm showed the peak at 575 nm (Figure 4). We hypothesize that different nonradiative pathways are sensed by the ensemble of chromophores in the two different experimental conditions. In addition, a spectral modification of the spectrum was observed during the measurements with a mean power density of 2.5 W/cm^2, and the emission spectra were sequenced by reducing the excitation power density to about 0.1 W/cm^2 and recording the data every 2 s over a cumulative period of 200 s of irradiation.

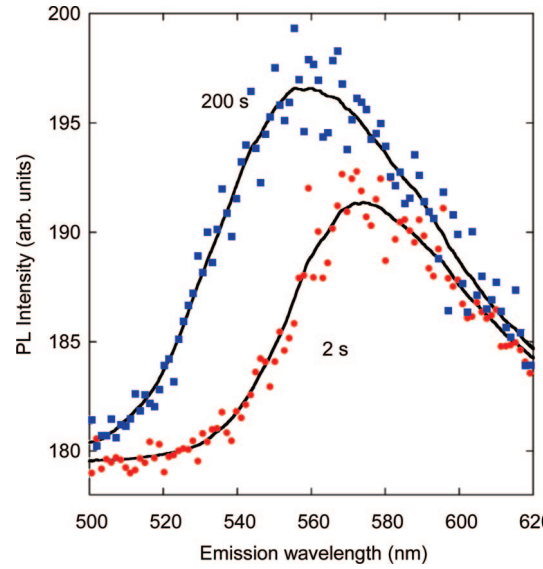

Figure 4. PL band at different irradiation doses.

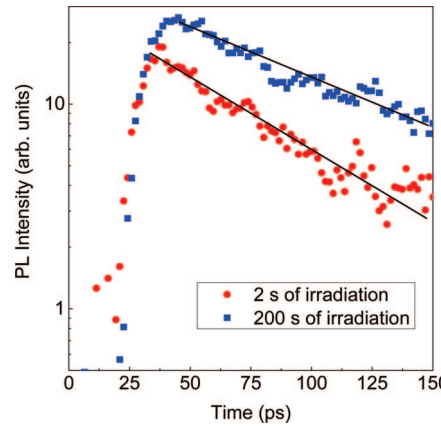

Figure 5. Time decays of the integrated emission band. Zero time irradiation (2 s) and 200 s of cumulative irradiation (solid lines are fitting results).

The PL spectra reported in Figure 4 refer to the emission at the experimental time zero (an accumulation time of 2 s was selected in order to obtain a good signal-to-noise ratio) and to the emission after the cumulative exposure of 200 s. The two spectra clearly show that the irradiation induced modifications of the PL features: the emission band was centered at about 575 nm as the experiment started and blue shifted to about 558 nm at the end of the measurement. The overall PL amplitude increases during the irradiation, but the contribution to the PL spectrum above 580 nm does not change during the irradiation time.

In Figure 5 the decay times of the PL intensity of the integrated emission at zero time irradiation and after 200 s of irradiation are reported. As expected, because of the large dye concentration, the estimated decay time is shorter than the typical values observed in less concentrated comparable systems or in solution, that is, tens of picoseconds instead of a few nanoseconds.[12−18,33]

It can be observed that the decay time of the emission recorded at the experimental time zero is shorter than the decay time of the emission gathered at the final irradiation dose. By fitting the experimental data with a single exponential decay, the values of 66.3 and 100.9 ps can be estimated for the integrated emission after 2 and 200 s of irradiation, respectively. These fast decays are due to typical quenching effects related

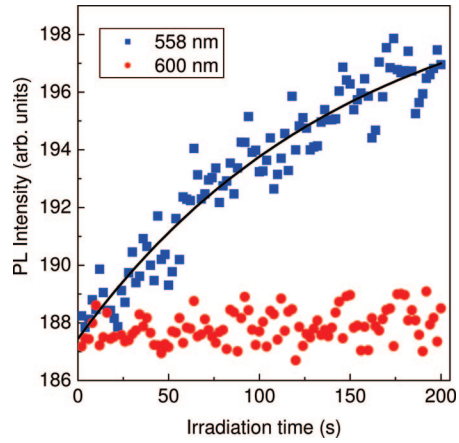

Figure 6. PL intensity at 558 and 600 nm as a function of cumulative irradiation time.

to the large concentration of the sample, that is, to the presence of molecular aggregates: comparable values of decay times were reported for dimer aggregates in concentrated water solutions of Rh6G.[31] However, the slight increase of the decay time after the cumulative irradiation dose is a clear indication of a modification of the nonradiative deexcitation pathways of the emission band.

The presence of nonfluorescent dimers and the fast decay time of the fluorescent species can be related to a very small value of the luminescence quantum yield.[11,37,38] A semiquantitative estimation of the quantum yield (QY) can be obtained by comparison with a standard reference, an ethanolic solution of Rh6G of 1×10^{-6} mol/L (QY = 0.98).[33] The estimated QY of the hybrid sample is <0.01, in agreement with previously reported values for highly concentrated systems.[31,37,38]

The recorded data clearly indicate the modifications of the spectroscopic features (peak position, decay time, and overall intensity) as a function of the cumulative dose of light irradiation. To our knowledge this is the first time that a light assisted increase of the PL efficiency and a blue shift of the emission peak are reported for this kind of sample. On the contrary, the typical effect of light irradiation is the photobleaching of the emitting dye molecules, which, up to now, has been the main obstacle to a large technological diffusion of hybrid samples in the photonic field. In addition, we would like to point out that the PL modifications under ultrafast excitation were not observed in samples with lower dye concentration.

It is worth noting that while the overall emission increases and the PL peak blue shifts as a function of the irradiation dose the contribution at larger wavelengths of the PL band is not decreased. This is an indication that the emission efficiency of the fluorescent aggregates is not affected by the irradiation. Figure 6 reports the increase of the PL signal recorded at 558 nm as the time irradiation increases; the trend of the emission gathered at 600 nm is also reported for comparison (the capacitor-like solid line is the fitting curve according to the model described in the following).

It is well-known that the molecules adsorbed on the porous silica surface keep a certain degree of mobility.[6,8,39−42] In addition, it was reported in the literature[6] that dimer aggregates can be separated into monomer units by thermal treatment. We propose to model the reported spectroscopic features as the light assisted transformation of dimers (both fluorescent and nonfluorescent) into monomers. This transformation can explain the increase of the PL intensity, the blue shift of the PL peak, and the increase of the PL decay time due to the reduction of the nonradiative pathways.

Let M and D the monomer and dimer species, respectively. The optically stimulated dimer to monomer transformation can be expressed by the following reaction:

$$\mathrm{D} \rightleftarrows 2\mathrm{M} \tag{1}$$

where the arrows indicate that at thermodynamic equilibrium the reaction proceeds in both directions with the same rate. Two different kinds of monomeric reaction products can be expected: a pair of independent monomers (free state) or a pair of correlated monomers, where the two molecules are separated but not completely free from one other (bound-like state). In such a case the correlated pair can be indicated as $\overline{\mathrm{MM}}$ and eq 1 is rewritten as

$$\mathrm{D} \rightleftarrows \overline{\mathrm{MM}} \tag{2}$$

The time-dependent kinetics of the emission can discriminate among the two species. In the case of independent monomers the rate equations of the hypothesized reaction can be expressed as follows:

$$\frac{\mathrm{d}n_{\mathrm{D}}}{\mathrm{d}t} = -\gamma I_{\mathrm{e}} n_{\mathrm{D}} + \eta(n_{\mathrm{M}}^2 - n_{\mathrm{M},0}^2) \tag{3}$$

$$\frac{\mathrm{d}n_{\mathrm{M}}}{\mathrm{d}t} = -2\eta(n_{\mathrm{M}}^2 - n_{\mathrm{M},0}^2) + 2\gamma I_{\mathrm{e}} n_{\mathrm{M}} \tag{4}$$

where n_{M} (cm^{-3}) and n_{D} (cm^{-3}) stand for the M and D concentrations, respectively, I_{e} ($\mathrm{cm}^{-3}\mathrm{s}^{-1}$) stands for the excitation light intensity, γ (cm^{-3}) stands for the cross section of dimer dissociation (including absorption cross section), and η ($\mathrm{cm}^{-3}\,\mathrm{s}^{-1}$) stands for the probability factor of the dimer formation. The ηn_{M}^2 term accounts for the aggregation rate of independent monomers, while the $\eta n_{\mathrm{M},0}^2$ term accounts for the reverse process at the equilibrium state. By assuming an Arrhenius-like thermal dissociation process, the latter can be expressed as follows:

$$\eta n_{\mathrm{M},0}^2 = s n_{\mathrm{D},0} \mathrm{e}^{-E/kT} \tag{5}$$

E is the activation energy of the thermal process and s is an appropriate frequency factor.

Equations 3 and 4 are not independent since

$$\frac{\mathrm{d}n_{\mathrm{M}}}{\mathrm{d}t} = -2\frac{\mathrm{d}n_{\mathrm{D}}}{\mathrm{d}t} \tag{6}$$

and the following condition is required:

$$n_{\mathrm{M}} - n_{\mathrm{M},0} = -2(n_{\mathrm{D}} - n_{\mathrm{D},0}) \tag{7}$$

The solution of the nonlinear kinetic equations can be presented in an implicit form, that is

$$\Delta n_{\mathrm{M}}(t) = \Delta n_{\mathrm{M,S}}\{1 - \exp[\alpha t - 2\eta \int_0^t \Delta n_{\mathrm{M}}(t')\,\mathrm{d}t']\} \tag{8}$$

where

$$\Delta n_M(t) = n_M(t) - n_{M,0};$$
$$\alpha = -[\gamma I_e + 2\eta(n_{M,0} + n_{M,S})] \quad (9)$$

The additional subscript "S" labels stationary state concentrations.

In the case of a pair of correlated monomers the rate equations have a linear form and can be written as follows:

$$\frac{dn_D}{dt} = -\gamma I_e n_D + \xi(n_M - n_{M,0}) \quad (10)$$

$$\frac{dn_M}{dt} = -2\xi(n_M - n_{M,0}) + 2\gamma I_e n_D \quad (11)$$

where ξ (s^{-1}) stands for the probability factor of the dimer formation from associated monomer pairs.

The easy solution is

$$\Delta n_M(t) = \Delta n_{M,S}[1 - \exp(-t/\tau)] \quad (12)$$

with

$$\tau = \frac{1}{\gamma I_e + 2\xi} \quad (13)$$

The solution for the correlated monomer problem is the typical capacitor charge-like equation (monomolecular kinetics). On the contrary, if compared to eq 12, the integral term in the exponential of eq 8 causes an anticipated saturation (bimolecular kinetics). Therefore, the time-dependent increase of the emission at 558 nm reported in Figure 6 allows discrimination among the possible results of the proposed reaction. Data can be successfully fitted with the capacitor charge-like equation (eq 12), while the use of eq 8 leads to a nonphysical value of the probability of the dimer formation ($\eta < 0$). The calculated time constant is about 150 s (fitting square correlation factor $R^2 > 0.98$). It should be noted that the exponential kinetics could also be explained by assuming that the formed monomers were not subjected to the reverse transformation in dimer pairs. We verify that this is not the case since the original emission of the sample was recovered in a time range comparable with the time constant deduced from the monomolecular kinetics (about 500 s). Thus, the exponential trend of the reported kinetics can be explained by assuming that the light assisted dimer to monomer transformation produces a pair of correlated monomers.

The reported light assisted modification of the spectral properties of the hybrid sample could have interesting technological applications: in the field of solid state lasers, for example, the mechanism can be useful to increase the density of monomer species in samples with a large concentration of dye molecules, in order to increase the emission efficiency or to extend wavelength tunability. In addition, since the monomer to dimer reverse transformation is thermally driven, one can hypothesize freezing the system once the light assisted transformation is concluded to store the information on the sample, realizing in this way an optical memory.

4. Conclusions

The spectral properties of heavily doped Rhodamine 6G porous silica hybrids are reported to discuss the aggregation of the dye molecules at the concentration limit. The reported features indicate the presence of both fluorescent (J) and nonfluorescent (H) dimers. By exciting the samples with ultrafast radiation, the light assisted transformation of both fluorescent and nonfluorescent dimers into fluorescent monomer species was observed. The modifications of the spectroscopic features were analyzed on the basis of a thermodynamic model to explain the kinetics of the dimer to monomer transformation. The model allowed demonstrating that the products of the reaction are pairs of correlated monomers.

References and Notes

(1) Drexhage, K. H. *Laser Focus* **1973**, *9*, 35–39.
(2) Lo, D.; Lam, S. K.; Ye, C.; Lam, K. S. *Opt. Commun.* **1998**, *156*, 316–320.
(3) *Sol-Gel Science and Technology, Processing, Characterisation and Applications*; Sakka, S., Ed.; Kluwer Academic Publishers: Boston, Dordrecht, 2005.
(4) Makishima, A.; Tani, T. *J. Am. Ceram. Soc.* **1986**, *69*, C-72–C-74.
(5) Narang, U.; Bright, F. V.; Prasad, P. N. *Appl. Spectrosc.* **1993**, *47*, 229–234.
(6) Innocenzi, P.; Kozuka, H.; Yoko, T. *J. Non-Cryst. Solids* **1996**, *201*, 26–36.
(7) Malashkevich, G. E.; Poddeneznyi, E. N.; Zelnichenko, I. M.; Prokopenko, V. B.; Demyanenko, D. V. *Phys. Solid State* **1998**, *40*, 427–431.
(8) Hungerford, G.; Suhling, K.; Ferriera, J. A. *J. Photochem. Photobiol., A: Chem.* **1999**, *129*, 71–80.
(9) Zhu, X.-L.; Lam, S.-K.; Lo, D. *Appl. Opt.* **2000**, *39*, 3104–3107.
(10) Rao, A. P.; Rao, A. V. *Mater. Lett.* **2003**, *57*, 3741–3747.
(11) Selwyn, J. E.; Steinfeld, J. I. *J. Phys. Chem.* **1972**, *76*, 762–774.
(12) Del Monte, F.; Ferrer, M. L.; Levy, D. *Langmuir* **2001**, *17*, 4812–4817.
(13) Reisfeld, R.; Zusman, R.; Cohen, Y.; Eyal, M. *Chem. Phys. Lett.* **1988**, *147*, 142–147.
(14) Avnir, D.; Levy, D.; Reisfeld, R. *J. Phys. Chem.* **1984**, *88*, 5956–5959.
(15) Del Monte, F.; Levy, D. *J. Phys. Chem. B* **1998**, *102*, 8036–8041.
(16) Del Monte, F.; Levy, D. *J. Phys. Chem. B* **1999**, *103*, 8080–8086.
(17) Del Monte, F.; Mackenzie, J. D.; Levy, D. *Langmuir* **2000**, *16*, 7377–7382.
(18) Ferrer, M. L.; Del Monte, F.; Levy, D. *Langmuir* **2003**, *19*, 2782–2786.
(19) Yariv, E.; Schultheiss, S.; Saraidarov, T.; Reisfeld, R. *Opt. Mater.* **2001**, *16*, 29–38.
(20) Knobbe, E. T.; Dunn, B.; Fuqua, P. D.; Nishida, F. *Appl. Opt.* **1990**, *29*, 2729–2733.
(21) Deshpande, A. V.; Namdas, E. B. *Chem. Phys. Lett.* **1996**, *263*, 449–455.
(22) Weiss, A. M.; Yariv, E.; Reisfeld, R. *Opt. Mater.* **2003**, *24*, 31–34.
(23) Costela, A.; Garcia-Moreno, I.; Figuera, J. M.; Amat-Guerri, F.; Sastre, R. *Appl. Phys. Lett.* **1996**, *68*, 593–595.
(24) Abedin, K. M.; Alvarez, M.; Costela, A.; Garcia-Moreno, I.; Garcia, O.; Sastra, R.; Counts, D. W.; Webb, C. E. *Opt. Commun.* **2003**, *218*, 359–363.
(25) Valverde-Aguilar, G. *Opt. Mater.* **2006**, *28*, 1209–1215.
(26) Eggeling, C.; Volkmer, A.; Seidel, C. A. M. *ChemPhysChem* **2005**, *6*, 791–804.
(27) Zondervan, R.; Kulaer, F.; Kol'chenko, M. A.; Orrit, M. *J. Phys. Chem. A* **2004**, *108*, 1657–1665.
(28) Hoogenboom, J. P.; van Dijk, E. M. H. P.; Hernando, J.; van Hulst, N. F.; Garcia-Parajo, M. *Phys. Rev. Lett.* **2005**, *95*, 097041-1–097041-4.
(29) Zondervan, R.; Kulser, F.; Orlinskii, S. B.; Orrit, M. *J. Phys. Chem. A* **2003**, *107*, 6770–6776.
(30) Carbonaro, C. M.; Anedda, A.; Grandi, S.; Magistris, A. *J. Phys. Chem. B* **2006**, *110*, 12932–12937.
(31) Penzkofer, A.; Leupacher, W. *J. Lumin.* **1987**, *37*, 61–72.
(32) Geltech technical report and U.S. Patent 5,076,980.
(33) *Dye Lasers*; Shaefer, F. P., Ed.; Topics in Applied Physics 1; Springer-Verlag: Berlin, 1973.
(34) Kemnitz, K.; Tamai, N.; Yamazaki, I.; Nakashima, N.; Yoshihara, K. *J. Phys. Chem.* **1986**, *90*, 5094–5101.
(35) Kemnitz, K.; Yoshihara, K. *J. Phys. Chem.* **1991**, *95*, 6095–6104.
(36) McRae, E. G.; Kasha, M. *J. Chem. Phys.* **1958**, *28*, 721–722.

(37) Bojarski, P.; Matczuk, A.; Bojarski, C.; Kawski, A.; Kuklinski, B.; Zurkowska, G.; Diehl, H. *Chem. Phys.* **1996**, *210*, 485–499.
(38) Bojarski, P. *Chem. Phys. Lett.* **1997**, *278*, 225–232.
(39) Narang, U.; Wang, R.; Prasad, P. N.; Bright, F. V. *J. Phys. Chem.* **1994**, *98*, 17–22.
(40) Bentivegna, F.; Canva, M.; Brun, A.; Chaput, F.; Boilot, J.-P. *J. Sol-Gel Sci. Technol.* **1997**, *9*, 33–39.
(41) Ferrer, M. L.; del Monte, F.; Levy, D. *J. Phys. Chem. B* **2001**, *105*, 11076–11080.
(42) Del Monte, F.; Ferrer, M. L.; Ley, D. *J. Mater. Chem.* **2001**, *11*, 1745–1751.

JP810835J